N. Olischläger, T. Preusser, M. Rumpf
[olischlaeger, preusser, rumpf]@uni-duisburg.de

Transport and Anisotropic Diffusion in Timedependent Flow Visualization

Duisburg University

Numerical Simulation and Scientific Computing

1 Introduction

Our aim is to visualize transport phenomena governed by timedependent vector fields. We expand and generalize an anisotropic diffusion method to allow for a multiscale visualization of longtime, complex transport problems. This process obeys a nonlinear transport diffusion equation with typically dominant transport. Starting from some initial noisy image, diffusion actually generates and enhances patterns which are then transported in the direction of the flow field. Simultaneously the image is sharpend in the direction orthogonal to the flow field. A finite element discretization in space and a semi implicit upwind scheme in time are applied to solve the transport diffusion PDE numerically.

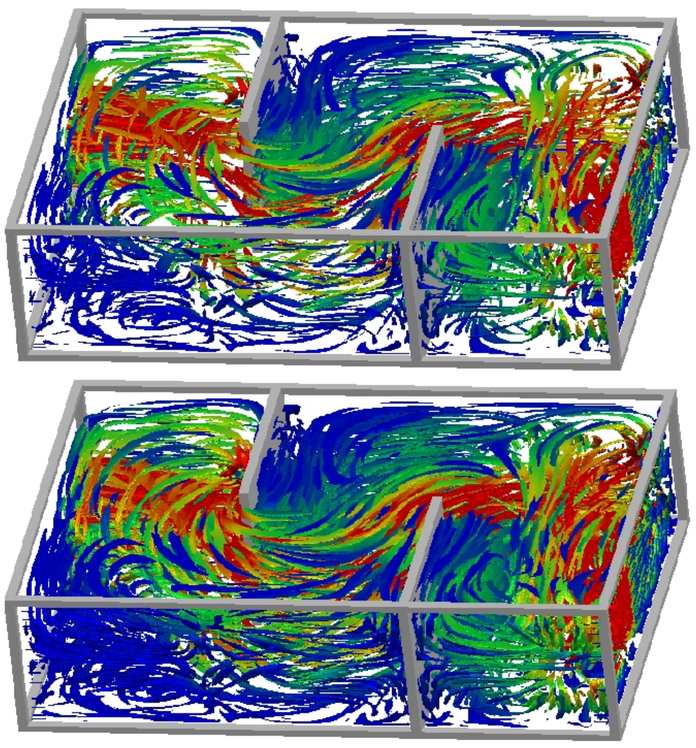

Fig. 1: Visualization of a 3D flow in a box. Color codes the velocity.

2 The Anisotropic Diffusion Method

An initial noisy image ρ_0 is smoothed along the streamlines of a given vector field $v : \Omega \to \mathbb{R}^d$ on a domain Ω , whereas the image is sharpened in the orthogonal direction by a Perona-Malik type diffusion. For steady flow fields, we solve the parabolic boundary initial value problem

$$\begin{aligned} \partial_t \rho + \nabla\rho \cdot v - \text{div}\,(A(v, \nabla\rho_\epsilon)\nabla\rho) &= f(\rho) && \text{on } \mathbb{R}^+ \times \Omega, \\ (A\nabla\rho) \cdot \nu &= 0 && \text{on } \mathbb{R}^+ \times \partial\Omega, \\ \rho(0, \cdot) &= \rho_0 && \text{in } \Omega, \end{aligned}$$

with a diffusion tensor $A(\nabla\rho_\sigma)$ depending on the vector field v defined in coordinates of $\{v, v^\perp\}$ by

$$A(v, \nabla\rho_\sigma) = (v, v^\perp) \begin{pmatrix} \alpha(\|v(x)\|) & 0 \\ 0 & G(\nabla\rho_\sigma) Id_{d-1} \end{pmatrix} (v, v^\perp)^T$$

with e.g. $G(s) = \frac{1}{1+s^2/\lambda^2}, \lambda \in \mathbb{R}$. The role of the right hand side f is to ensure contrast enhancement. The coefficient $\alpha : \mathbb{R}^+ \to \mathbb{R}^+$ controls the linear diffusion in vector field direction, i. e. along streamlines, and the edge enhancing diffusion coefficient $G(\cdot)$ acts in the orthogonal directions.

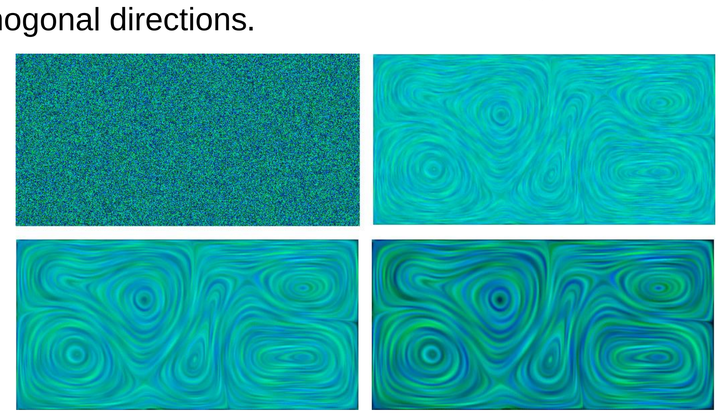

Fig. 2: Successive scale steps of the visualization of a Bènard convective flow.

3 A Transport Diffusion Model

The above reviewed anisotropic diffusion method visualizes the vector field freezed at time t but offers only very limited insight in the actual transport process governed by the underlying time-dependent flow field. Analysing the true transport problem and its particle lines respectively, we obtain as a conservation law the vanishing of the material derivate

$$\frac{D}{dt}\rho := \frac{\partial\rho}{\partial t} + \nabla\rho \cdot v = 0.$$

Finally, our transport diffusion model for timedependent vector field looks as follows:

$$\partial_t \rho + \nabla\rho \cdot v - \text{div}\,(A(v, \nabla\rho_\epsilon)\nabla\rho) = f(\rho) \quad \text{on } \mathbb{R}^+ \times \Omega,$$

where $A(v, \nabla\rho_\epsilon)$ is the diffusion tensor from the anisotropic diffusion for steady flow fields. This model then generates and stretches patterns along the flow field and transports them simultaneously.

4 Balancing Parameters

In general, transport and diffusion are contrary processes. The diffusion could overrun the transport. Hence, we interduce a balancing parameter $\beta \in \mathbb{R}^+$ to control the diffusion. A suitable diffusion coefficient will be:

$$\alpha(\|v\|) = \frac{\beta^2 \|v(x)\|^2 \tau}{2}$$

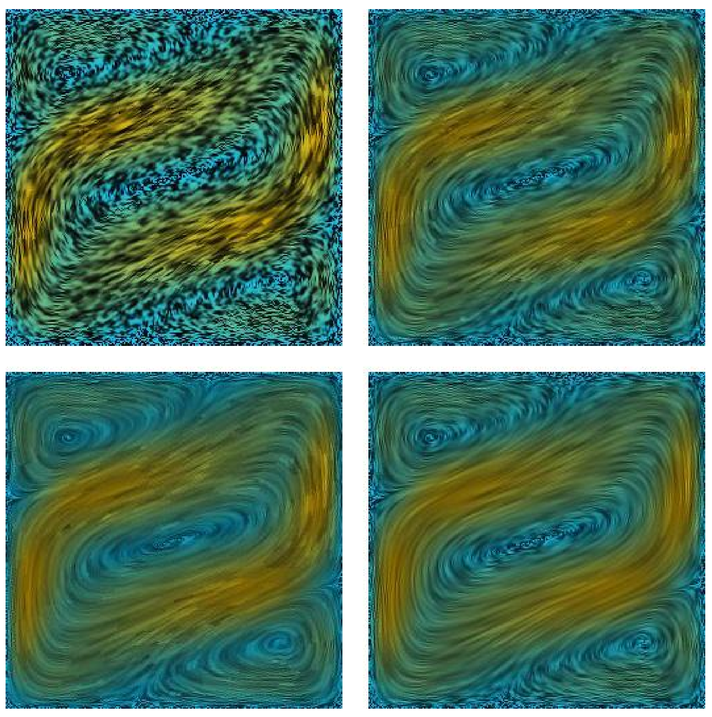

Fig. 3: One time-step of the transport diffusion process generating directed patterns of a Bénard convection for different choices of β and λ is shown. The additional coloring indicates the speed of the flow field.

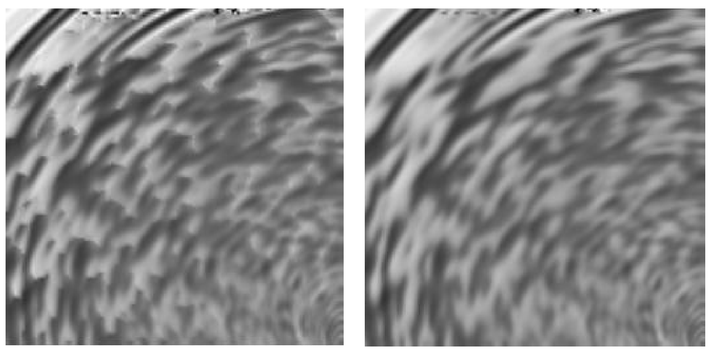

Fig. 4: Zoomed images of patterns generated for a circulating flow are depicted. On the left directed patterns are generated based on the incorporated "one–sided" diffusion and on the right the original model with linear diffusion along motions paths is depicted.

5 Generating Directed Patterns

The above discussed balancing of parameters with respect to a dominated transport does not completely diminish diffusion effects downstream. At least at the "head" of the evolving pattern a slight modification of the proposed model helps to avoid this misleading drawback. Hence, we incorporate a "one–sided" diffusion i. e. we replace the tangential diffusivity $\alpha(v)$ by

$$\alpha(v, \nabla\rho) = \begin{cases} \alpha_{\max}\, G\left((\nabla\rho \cdot v)_+\right) & \text{if } \rho \le 0.5, \\ \alpha_{\max} & \text{else,} \end{cases}$$

which depends in addition on the evolving intensity. Then lighter pattern will not diffuse downstream and a sharp front at the top of the pattern together with a typically blurred intensity in the upstream direction will underline the direction of the flow.

6 Discretization

For the discretization of the above transport diffusion problem we pick up an algorithm due to Pironneau for the discretization of transport dominated problem. Furthermore, for the diffusive term of the equation we apply a semi-implicit scheme, where the diffusion coefficient $G(\cdot)$ and the right hand side $f(\cdot)$ are evaluated at the previous time-step. Let us indicate by an upper index n the time-step and by τ the time-step size. Then, a suitable approximation of the material derivative at time $t_n = n\,\tau$ is given by

$$\frac{D}{dt}\rho(t_n, \cdot) \approx \frac{\rho^{n+1} - \rho^n \circ X^n}{\tau},$$

where X^n is a numerical 2^{nd} order upwind integration of the velocity field. Therefore we obtain as variational formulation:

$$\begin{aligned} \left(\frac{\rho^{n+1} - \rho^n \circ X^n}{\tau}, \theta\right) + \left(A(v, \nabla\rho_\epsilon^n \circ X^n)\nabla\rho^{n+1}, \nabla\theta\right) \\ = (f(\rho^n \circ X^n), \theta) \qquad \forall\theta \in C^\infty(\Omega), \end{aligned}$$

where $(\cdot, \cdot)$ denotes the L^2 scalar product on Ω. A spatial finite element discretization using multilinear basis functions on regular grids can be easily derived.

7 Long Term Animation

For long term animation purposes we select a suitable window for the involved scale parameter and use blending techniques to provide a dense pattern motion in the selected scale range at any time.

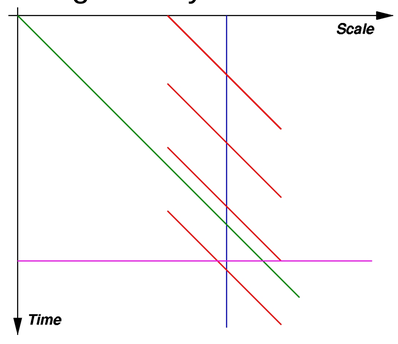

Fig. 5: A schematic sketch of the general relation between scale and time parameter in our combination of image processing and flow computation is depicted. We compare the case of varying scale for steady state flow fields at fixed time (magenta), the simultaneously time and scale evolution (green), the optimal but non practical case of a fixed scale for varying time (blue) and our blending approach (red).

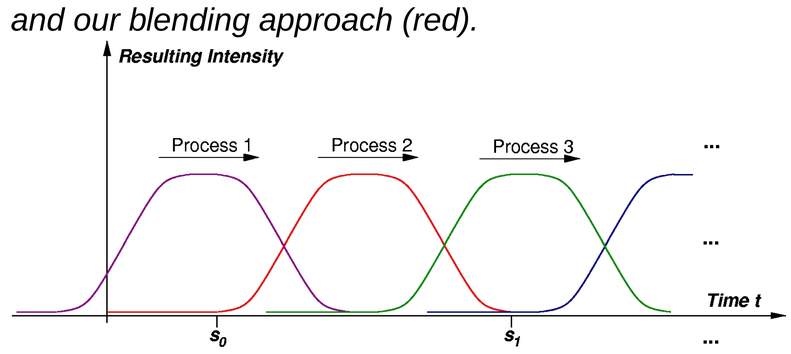

Fig. 6: The weighting factors in the blending operation together with the overlapping scale/time intervals of the considered transport diffusion processes are shown in a diagram over time.

8 Bibliography

[1] D. Bürkle, T. Preusser and M. Rumpf. *Transport and Anisotropic Diffusion in Timedependent Flow Visualization.* Proceedings Visualization 2001

[2] T. Preusser and M. Rumpf. *Anisotropic Nonlinear Diffusion in Flow Visualization.* Proceedings Visualization 1999

[3] J. Becker, T. Preusser, and M. Rumpf. *PDE methods in flow simulation post processing.* Computing and Visualization in Science, 3(3):159-167, 2000.

[4] `http://numerik.math.uni-duisburg.de/exports/tdFlowVis/`